Journal of ELECTRONIC MATERIALS, Vol. 48, No. 11, 2019
https://doi.org/10.1007/s11664-019-07172-z
© 2019 The Minerals, Metals & Materials Society

Effects of Aging and Environmental Factors on Performance of CdTe and CIS Thin-Film Photovoltaic Modules

MEHMET DEMIRTAŞ ,[1,4] BÜNYAMIN TAMYÜREK,[2] EROL KURT,[1] İPEK ÇETINBAŞ,[2] and MUSTAFA KEMAL ÖZTÜRK[3]

1.—Department of Electrical and Electronics Engineering, Faculty of Technology, Gazi University, 06500 Beşevler, Ankara, Turkey. 2.—Department of Electrical and Electronics Engineering, Faculty of Engineering and Architecture, Eskişehir Osmangazi University, 26480 Eskisehir, Turkey. 3.—Department of Physics, Faculty of Science, Gazi University, 06500 Beşevler, Ankara, Turkey. 4.—e-mail: mehmetd@gazi.edu.tr

The effects of aging and environmental factors on the performance of cadmium telluride (CdTe) and copper indium gallium selenide (CIS) thin-film photovoltaic (PV) modules have been analyzed. Recent developments in thin-film technology have resulted in reduced manufacturing costs and increased cell efficiency, making thin-film PV modules desirable for future solar-energy-generation systems. Such PV modules are currently used for various power system applications; however, their performance during the operational lifetime is greatly affected by aging and module failures caused by environmental factors. In this study, x-ray diffraction and infrared radiation imaging were used to characterize the imperfect surfaces of CdTe and CIS samples taken from a real application under various aging and environmental conditions. The performance of the modules was also evaluated by measuring the current, voltage, power, and efficiency over 3.5 years. During this period, we mainly detected corrosion, delamination, micro-cracks, and hot-spot failures. At the end of the study, the module degradation factors (MDFs) were calculated based on the measured results. The micro-crack and delamination failures resulted in MDFs of 14.49% for the CdTe modules and 21.24% for the CIS modules. With these MDFs, the installed system inevitably experienced substantial power loss in generation: 21.7% for the CdTe modules and 31.5% for the CIS modules. Consequently, our findings indicate that the performance of a PV system is susceptible to aging, meteorological conditions, and the PV technology; these factors should thus be considered before implementing PV system designs to achieve the most efficient and cost-effective power generation.

Key words: Thin film solar module, PV module failure, delamination, corrosion, module efficiency, module degradation factor

INTRODUCTION

The significant increase in electric energy consumption worldwide suggests a corresponding substantial increase in the demand for energy generation. According to a study performed by the Organization for Economic Cooperation and Development (OECD) group, the energy consumption of OECD countries was 957.5 TWh in January 2018, representing an increase of 3% compared with that in January 2017, which is a significant increase in 1 year. Renewable sources such as solar and wind energy take up a share as high as 32.8% within this 3% increase.[1] From these statistics and the ratio of renewables versus primary energy sources used for

(Received September 30, 2018; accepted March 25, 2019; published online April 19, 2019)

energy generation, we can conclude that renewables are becoming real alternatives.

Among renewable energy technologies, PV modules have been widely used for electricity generation in both residential and industrial applications, where a grid may or may not be available.[2] Of existing PV technologies, thin-film PV modules have become the preferred option for solar applications for the following reasons. First, thin-film PV modules yield the fastest payback time, and their efficiency is continually improving. Second, thin-film PV modules have low temperature coefficients during operation in the field, making them suitable for hotter environments. In addition to these advantages, thin-film PV technology is being continually developed, with superior electrical characteristics being achieved, thereby adding valuable contributions to conventional silicon PV module technology and finding widespread usage in the field.[3,4]

Various types of failures are likely to occur in PV modules over their operation lifetime that decrease the overall performance. Although module manufacturers generally provide a 10-year guarantee for their products, some module structures can still be damaged both physically and chemically, mainly because of climate and environmental factors. The most common factors causing this damage are prolonged operation under humid and hot climate conditions, instant temperature changes, problems associated with snow and ice, and corrosive environments. The defects and damage lead to degradation of the cell structure and reduction of the output power of the module. Any drop in output power is directly related to the economic value of the installation as the reduced performance results in reduced payback time.[5,6]

In general, failures in PV modules caused by environmental conditions can be classified as quick connector reliability, delamination, glass breakage, or junction box damage. These types of failures can occur in all types of modules. In wafer-based silicon modules, however, cell cracks, ethylene vinyl acetate discoloration, burn marks, potential induced degradation, fatigue of the ribbon due to thermal cycling, bypass diode failure, and light-induced cell degradation failures have been observed. During the manufacture of thin-film PV modules such as Si, cadmium telluride (CdTe) and copper indium gallium selenide (CIS) modules, they may develop shunt hot-spot failures due to either common production processes or the reverse front voltage operation. In addition to these failures, initial light degradation and annealing instabilities (amorphous silicon module) failures may occur in thin-film Si modules. For thin-film CdTe modules, cell layer integrity-back contact stability and busbar failure-mechanical (adhesion) and electrical failures may also be observed.[7] Some failures do not cause a significant efficiency loss; however, some may result in certain issues that make the module unusable. Although CIS modules have lower failure rates, the highest fault rates are encountered in CdTe modules. For Si samples, the failure rate is generally defined as 0.8% annually.[8]

Many studies have been performed on the failure types in PV modules and the associated effects of these failures on the module performance, such as the efficiency and reliability. For example, Muehleisen et al.[9] investigated three PV power stations affected and damaged by a hailstorm. They used outdoor electroluminescence and ultraviolet–fluorescence imaging methods to determine the damage in both the cells and modules caused by hail. In another investigation, Chandel et al.[10] studied the effect of degradation on monocrystalline silicon modules used for a solar-energy-supplied water pump after 28 years of continuous operation. They investigated the damage and defects in the modules and later evaluated them in terms of performance and reliability. Bouraiou et al.[11] studied and evaluated the failure and damage that occurred in monocrystalline and polycrystalline modules operated in a solar-energy power plant installed in a desert environment. They evaluated many failures such as the delamination and color change of the enclosure, and the results were used to improve the manufacturing process of PV modules to achieve improved lifetimes. Bandou et al.[12] investigated PV modules placed in a desert environment over 28 years. In this investigation, the cracks and hot-spot failures in the modules were analyzed, and the degradation in the power, short-circuit current, and open-circuit voltage over time was evaluated. In another study, Andenæs et al.[13] investigated the shading effect of ice and snow covering the surface of PV modules either partially or entirely. They also investigated the effect of the ice and snow covering on the energy production. Similarly, Silvestre et al.[14] investigated the failures of four thin-film PV modules operated in a dry and sunny region over a 5-year period. Tahri et al.[15] evaluated the failures that occurred in two types of thin-film PV modules operated in semi-dry climate conditions over a 3-year period. The annual failure rates were calculated and compared with the rates in different regions.

In a recent study, Demirtaş et al. analyzed and evaluated the failures in CdTe and CIS PV modules configured as a rooftop application at Gazi University Golbasi campus in Ankara, Turkey. During the 3.5-year evaluation period, they discovered corrosion, delamination, hot-spots, micro-cracks, and breakage failures in these modules and used infrared radiation (IR) imaging to analyze the failures.[16] Similarly, Kahoul et al.[17] studied the early degradation of PV modules operated in a desert region for 11 years. They determined the types of failures and estimated the rate of defects in cells in an experimental study. The current–voltage characteristics of the modules were classified in the analyses. They estimated 12% degradation in the

performance over the studied period. Quansah et al.[18] investigated the power losses of 29 crystalline silicon modules installed at six different locations after aging for 6–32 years for three different applications (water pumping, battery charging, and exploiting grid connection effects).

The research discussed in this paper is an extension of the work presented in Ref. 16. A detailed description of the thin-film PV arrays and a comparative analysis of these cell types in terms of output power and energy production capabilities are provided. In addition, a comparative analysis was performed based on x-ray diffraction (XRD) structural analysis of the CdTe thin-film PV arrays. Calculation of the module degradation factors is also included. The objective of this work was to provide a better understanding of the effect of climate and environmental conditions on the power production capability, current, and voltage parameters of the two types of thin-film PV modules. During the evaluation period, a substantial amount of data was collected from both damaged and undamaged modules for analysis and comparison. Five different types of failures were observed in the modules: corrosion, delamination, hot-spots, micro-cracks, and breakage. The failed CIS PV modules were investigated using IR imaging, and the damage in the CdTe PV modules was examined using XRD to determine the structural quality. In addition, the degradation factors of these two module structures were compared using real data.

THIN-FILM PV ARRAYS AND WORKING ENVIRONMENT

In this section, we first describe the basic cell structures of the CdTe and CIS PV modules and then provide efficiency information based on literature data and describe the two arrays constructed based on these modules. Finally, we explain the working environment of the arrays configured for the intended application. As shown in Fig. 1a, the basic structure of the CdTe-based thin-film PV cell consists of a glass substrate, transparent conducting oxide (TCO) layers such as SnO_2 or Cd_2SnO_4, intermediate layers such as CdS and CdTe layers, and a metal layer at the back to form electrical contacts. The CIS-based thin-film PV cell structure consists of ZnO, CdS, CIS, and Mo layers deposited on a glass, metal, or polymer substrate, as shown in Fig. 1b.[19] Many studies on PV cell structures have been conducted.[20] Efficiency studies on CdTe and CIS samples have been performed under the global AM1.5 spectrum at 1000 W/m^2 and 25°C both in a single-junction terrestrial cell and in a module. The efficiencies of the CdTe samples were measured to be 21.0 ± 0.4% for the cell-based measurements and 18.6 ± 0.5% for the module-based measurements. The efficiencies of the CIS samples were measured to be 21.7 ± 0.5% for the cell-based measurements and 19.2 ± 0.5% for the module-based measurements.[21] Thus, the CIS structure provides a higher energy conversion efficiency than the CdTe structure. In contrast to the CdTe module, which requires hard glass as the substrate, the CIS module can be easily applied to flexible surfaces. However, CdTe modules have lower manufacturing costs than CIS modules. The manufacturing cost of thin-film PV technology is always less than that of other types of modules. Therefore, thin-film modules can be mass-produced at much lower cost. In addition, thin-film modules are less affected by factors such as shading and temperature than other types of PV modules.[22,23]

Figure 2 shows the experimental working environment where the PV module strings were installed on the roof of an office building at Gazi University Golbasi Campus Technopark. Both the CdTe and CIS PV strings in Fig. 2 were installed on the same roof with an inclination angle of 40° facing the north–south direction. The electrical parameters of both modules were determined under standard test conditions at 1000 W/m^2 and are tabulated in Table I. The configuration of the strings and the electrical properties of the modules used in the strings are described below.

CdTe Thin-Film PV String The model number of the CdTe module was AB1-67. The module had a nominal power of 67.5 W and an efficiency of 9.38%. The string consisted of 30 modules connected in series to obtain a total power of 2025 W. The system

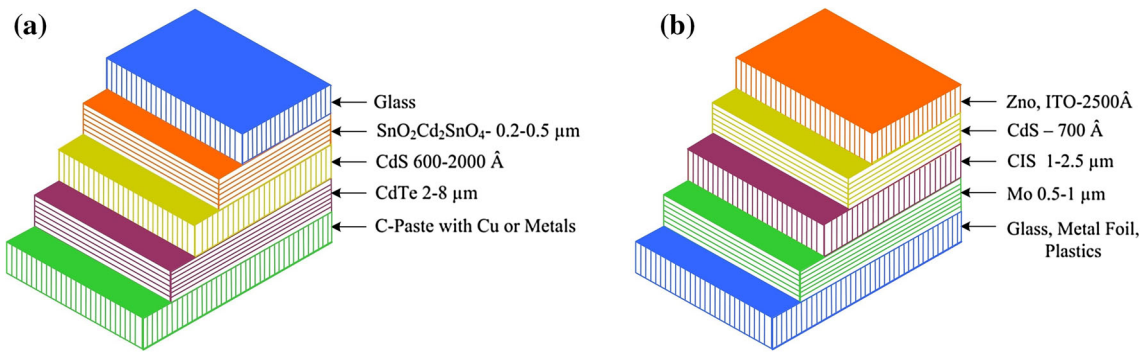

Fig. 1. Basic structures of thin film PV cells: (a) CdTe structure, (b) CIS structure.

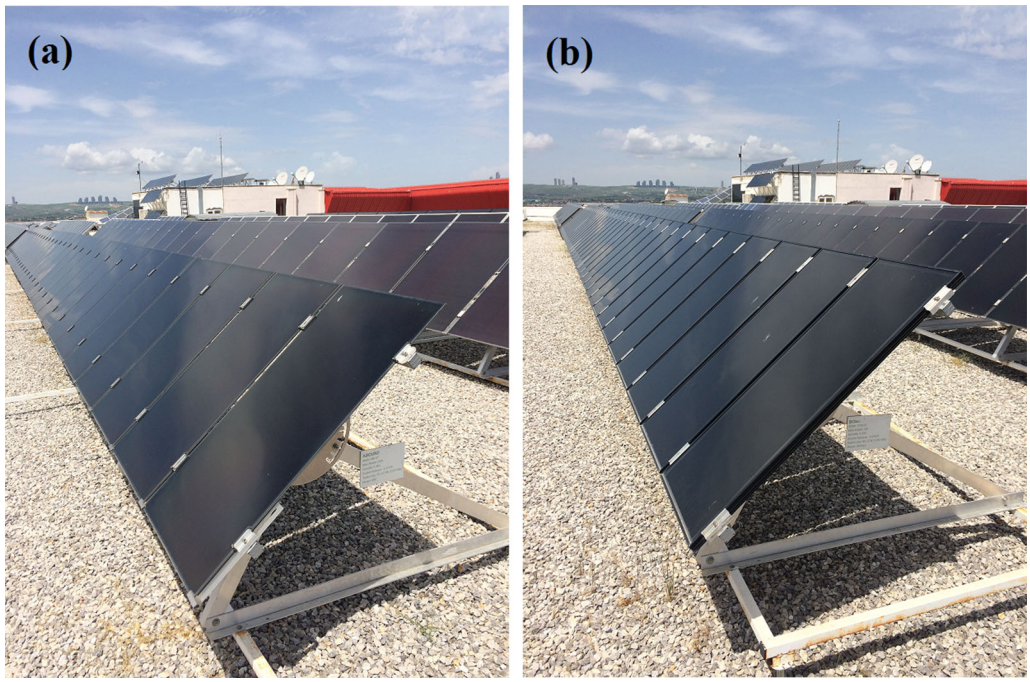

Fig. 2. Experimental setup at Gazi University Golbasi campus Technopark: (a) CdTe thin-film module string and (b) CIS thin-film module string.

Table I. Electrical parameters of modules

Module parameters	CdTe	CIS
Nominal power (W)	67.5	57
Voltage at P_{MPP} (V)	33.60	26.4
Current at P_{MPP} (A)	2.03	2.16
Open-circuit voltage (V)	46	34.4
Short-circuit current (A)	2.48	2.41
Temperature coefficient (%/K)	−0.37	−0.53
Total power (W)	2025	2052
Efficiency (%)	9.38	9.30
Country of origin	USA	Germany

was designed to operate with a 3-kW inverter in grid interactive mode.

CIS Thin-Film PV String The model number of the CIS module was C100-A1. The module had a nominal power of 57 W and an efficiency of 9.30%. The string consisted of 36 modules connected in series to obtain a total power of 2052 W. The system was also designed to operate with a 3-kW inverter in grid interactive mode.

The strings are thus comparable for evaluation purposes because the designs of strings from an electrical standpoint were almost identical.

RESULTS AND DISCUSSION

Comparative Analysis of PV Modules

In this study, both of the PV module strings were placed on the same roof with the same inclination angle to enable a fair comparison. The objective of this study was to analyze the failure types and compare the effects of failures on the performance and efficiency under the same environmental conditions. All the data were collected on a daily, monthly, and annual basis over a 3.5-year period beginning in January 2015 and ending in August 2018. The daily data, recorded at 5-min intervals, include the dc side current, voltage, and power, and the grid side ac current, voltage, power, and frequency. The monthly recorded data consisted of the energy production (kWh) were measured from the inverters to which the PV strings were connected.

As shown in Fig. 3, we observed delamination, hot-spot, and micro-crack failures in the PV modules during the examination period. The delamination and hot-spot failures shown in Fig. 3a and b were observed in the CIS modules, and the micro-crack failure shown in Fig. 3c was observed in the CdTe modules. These failures started appearing in July 2017 and became more prominent depending on the meteorological and environmental conditions.

The observed failures caused a reduction in the generated power and decreased efficiency. To analyze the effect of these failures on the overall performance, the module power production capability before and after the failures was evaluated. The power production before the failures was determined for a normal sunny day and a cloudy day to obtain a basis for future comparisons. Figure 4a presents a sample dc power production plot for both strings for a normal day, and Fig. 4b presents the same data for a cloudy day. It is apparent that the CIS modules performed more efficiently than the CdTe modules for the same inclination angle. The CIS modules also generated approximately three

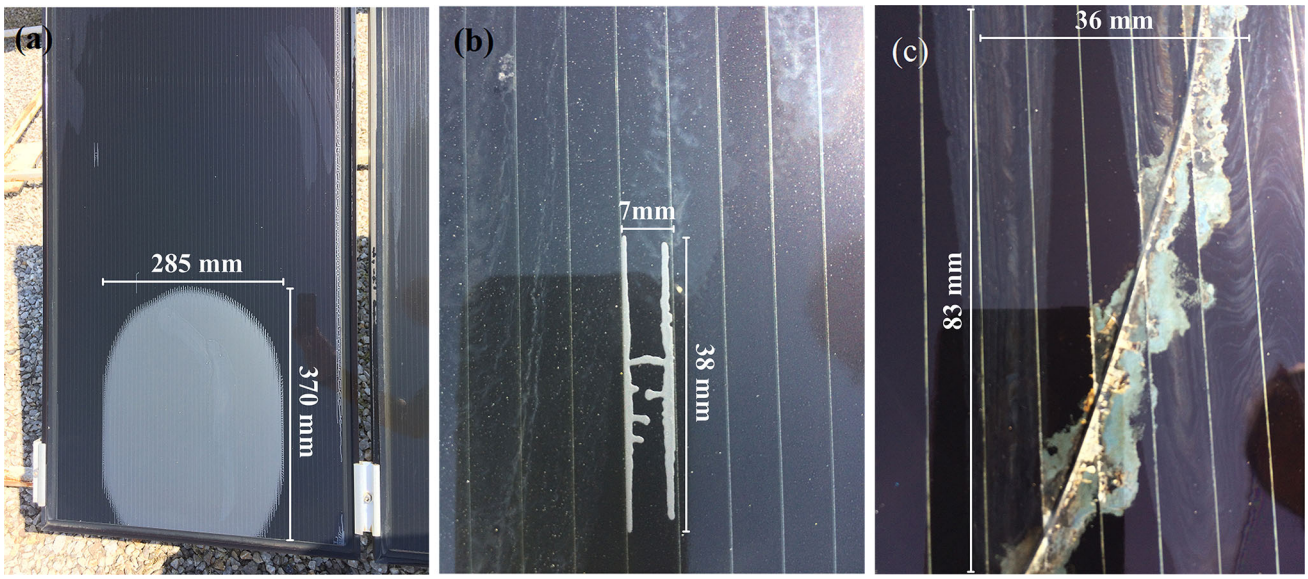

Fig. 3. Failures occurring in PV modules: (a) delamination, (b) hot spot, and (c) micro-crack.

times more power than the CdTe modules when considering the daily energy generation values.

The CdTe and CIS PV modules were theoretically analyzed and compared to understand the causes of the mismatch in power generation. The optical absorption coefficients of the CIS modules were much higher than those of the CdTe modules. In addition, the CIS modules could operate with higher efficiency under optimum radiation and temperature levels.

Figure 5 presents a plot of the dc power generation data of the strings after 1 year of operation. A decrease of 21.7% in the power generation of the CdTe string and a decrease of 31.5% in the power generation of the CIS string were observed in the same month within the same time interval after a 1-year period. We can thus conclude that the main reason for the drop of efficiency in the PV modules and corresponding decrease in the power generation was the failures in the modules. Comparison of the measurements over the entire exploration time reveals that the module failures were prominent after August 2017.

We used a FLIR IR camera to monitor and evaluate the failures occurring in the modules. Images of the delamination defects in the CIS modules are presented in Fig. 6. The regions of the delamination failures were colder than the other regions in the modules. The physical structures in these modules differed from the structures in monocrystalline modules, and these modules behaved more like a single cell structure than like modules consisting of multiple cell structures. Therefore, the heat loss at any point in the module or irradiation loss due to surface coverage affected the entire module.

Figure 7 presents IR images of the compared modules. The delamination failures in the CIS module string were easily detected because they created cold regions. However, the micro-cracks occurring on the CdTe module string were not visible. Thus, the IR imaging method could not be used to analyze the micro-crack failures, and failure detection of the CdTe modules was instead performed using XRD structural analysis. The results of these analyses are presented in the next section ("XRD Structural Analysis of CdTe Thin-Film PV Arrays" Section).

Monthly energy generation data of the CIS and CdTe strings over the 3.5-year period were also collected, and the power generation histories of the CIS and CdTe PV strings are shown in Fig. 8a and b, respectively. A noticeable decrease in the efficiency of the CIS modules was observed in the months after the failures started to occur. The decrease in the efficiency of the CdTe modules with micro-crack failures was relatively less pronounced than that of the CIS modules.

According to the data presented in Fig. 8a, the energy generation performance of the CIS PV modules started to decrease in 2017. A similar decrease in the power generation capability was observed during the first 8 months of 2018. In contrast, as observed in Fig. 8b, the efficiency loss in the CdTe-type modules was much lower, and these modules operated with almost the same efficiency in consecutive years. The total energy production values of the modules over the 3.5-year period were measured to be 12,794 kWh for the CIS modules and 2933 kWh for the CdTe modules. It is important to note that the modules had very similar efficiency specifications according to their catalog information even though the energy production differed substantially in the real working environment. Thus, our findings demonstrate that PV modules with the same theoretical efficiencies can

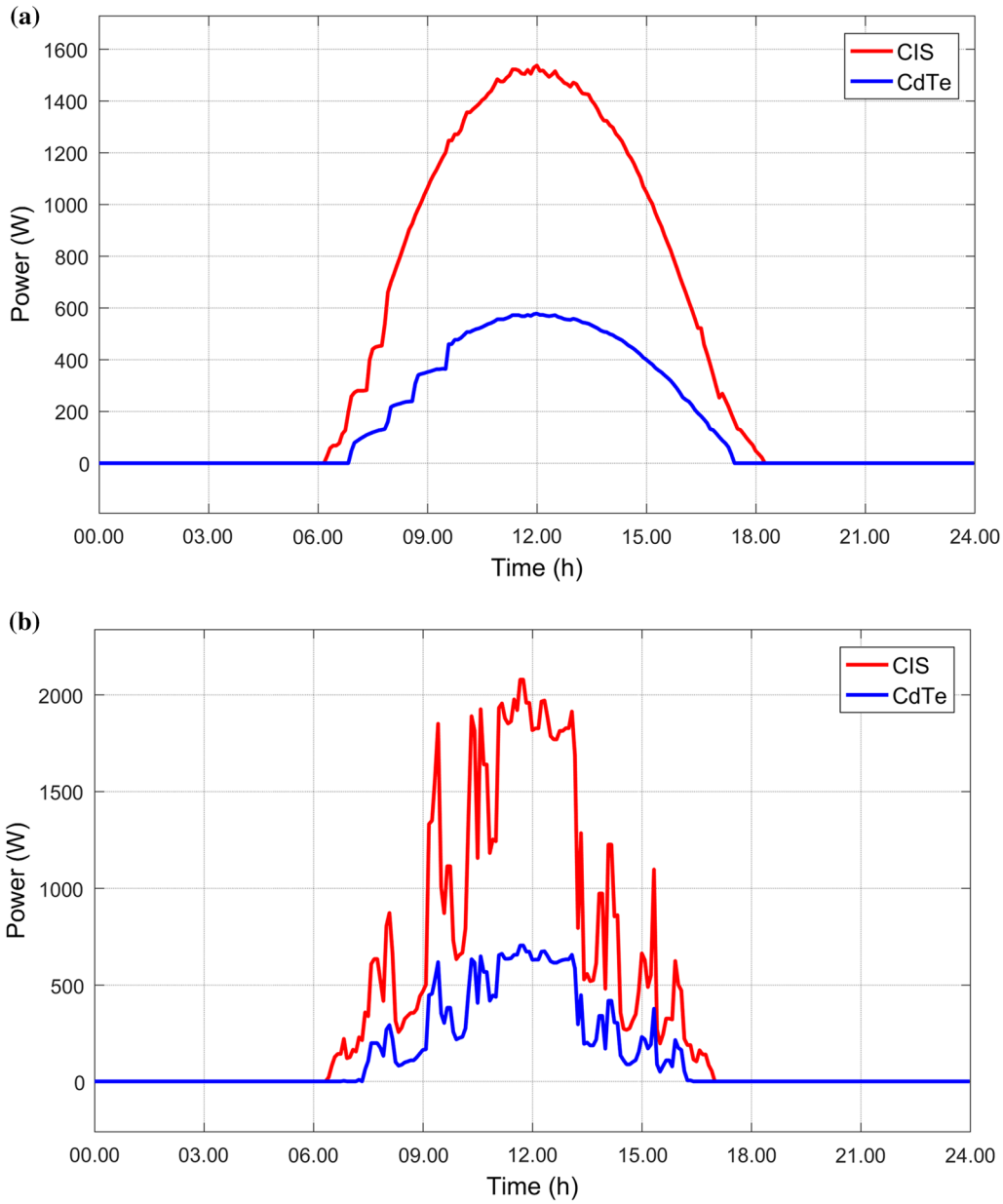

Fig. 4. PV string dc power generation data before module failures: (a) on a normal sunny day on July 1, 2016, and (b) on a cloudy day on October 15, 2016.

perform differently and exhibit different electrical characteristics under real working conditions.

XRD Structural Analysis of CdTe Thin-Film PV Arrays

The micro-crack failures of the CdTe modules were analyzed using XRD analysis. A GNR APD 2000 pro diffractometer with Theta–2Theta axis and Bragg–Brentano geometry and a fast detector was used for the XRD analysis. The XRD tube consisted of a Cu source with a wavelength of 1.5406 Å. The XRD results from the undamaged part of the commercial CdTe thin-film array are presented in Fig. 9. The (111), (220), (311), (040), (402), (242), and (511) peaks of Miller indices are consistent with those of the powder diffraction file (PDF) 96-900-8441, indicating that the CdTe had a cubic structure with a lattice parameter of 6.480 Å. These XRD results can also be compared with those of Ref. 24.

Structural analyses of three regions, especially around the crack of the CdTe PV, were also performed to analyze the structures of the defected regions. In addition, powder samples were collected from locations where the PV was broken to determine the environmental contaminants in the surface crack zone. XRD patterns of all the samples are presented in Fig. 10, and the XRD pattern of the powder is presented for the comparison in Fig. 10a.

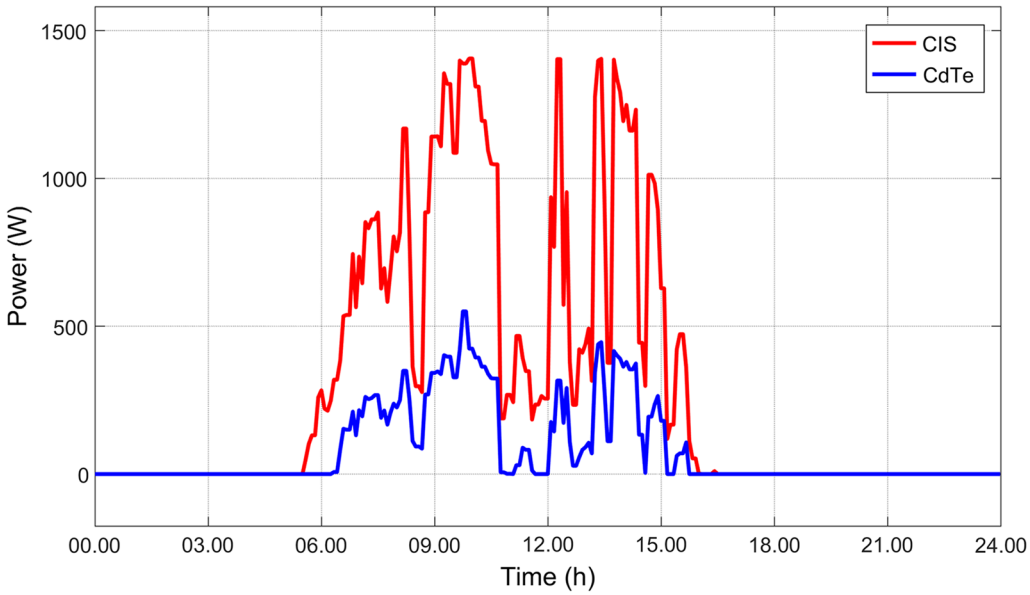

Fig. 5. PV string dc power generation with failed modules recorded on October 20, 2017.

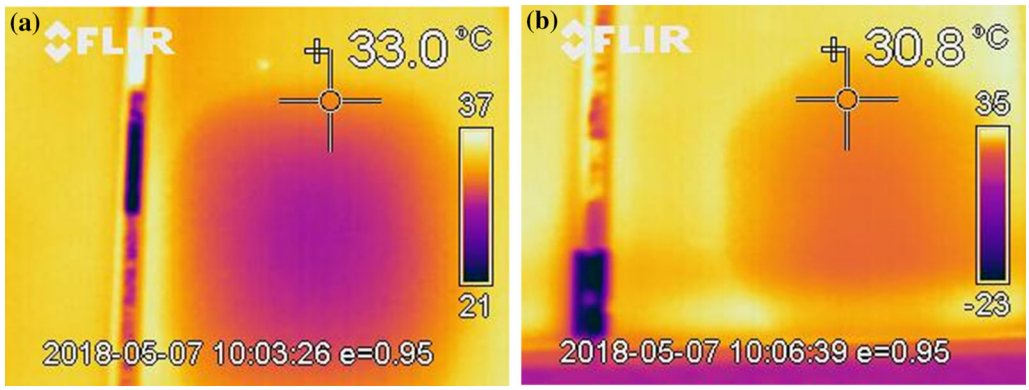

Fig. 6. Images of delamination defects on CIS modules taken using with an IR camera.

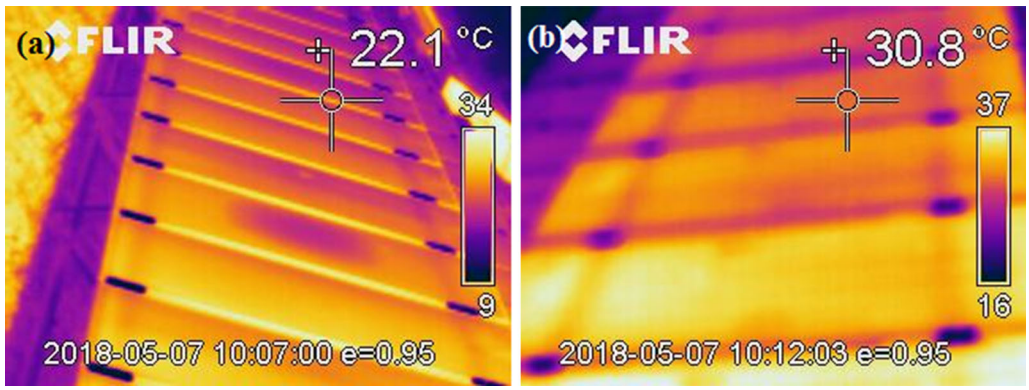

Fig. 7. IR camera images of thin-film PV module strings: (a) CIS and (b) CdTe.

The dust mainly consisted of quartz and calcite minerals according to the measurements. The XRD peak of the glass is visible at 26.530°. The calcite corresponds to PDF 01-074-0764 with a hexagonal structure and lattice parameters of $a = b = 4.9977$ Å and $c = 5.4601$ Å; the main peak in Fig. 10a at 26.2540° is indexed to the (101) plane. In addition, a (100) peak is observed at 20.5040°. The quartz was

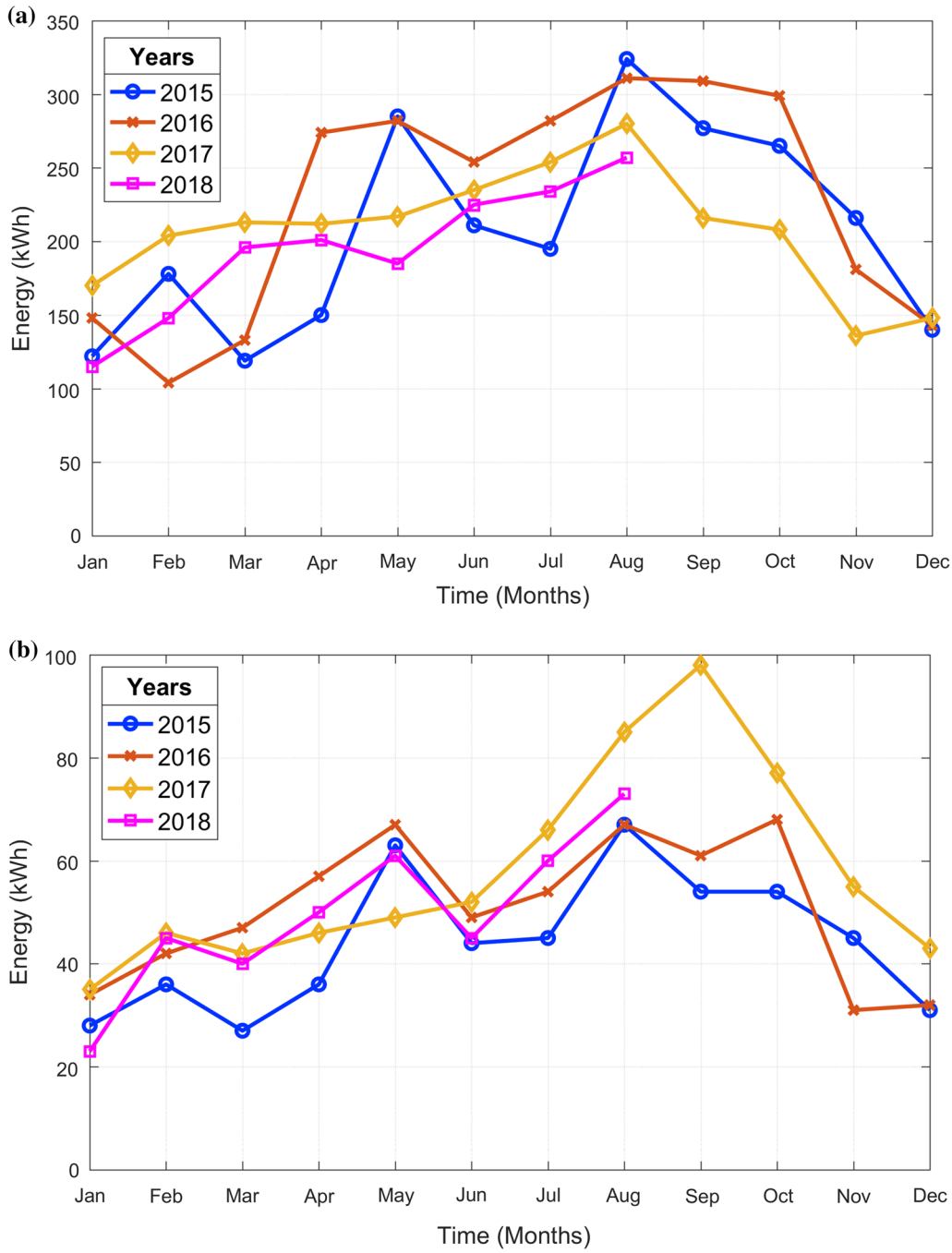

Fig. 8. Annual power generation data of PV strings: (a) CIS and (b) CdTe.

identified as PDF 01-086-0174 with $a = b = 4.9880$ Å and $c = 17.0680$ Å and a rhombohedral structure, and the main peak in Fig. 10a at 29.3990° is indexed to the (104) plane. The other (202) peak appeared at 43.3990°. The XRD patterns of the three different regions differed from each other, as observed in Fig. 10b. In the XRD pattern of the first damaged part, crystallized quartz was detected and appeared to be a grown layer. Comparison of the XRD patterns of the dust and damaged areas reveal that the peak intensities of the quartz and calcite XRD planes fluctuated on the imperfect surfaces, indicating the collected amount of dust on the surface. As a result of long-term damage, CdTe was not detected in the XRD pattern. Indeed, the CdTe was removed from the surface because of the moisture content on the damaged surfaces.

Analysis of Module Degradation Factors (MDFs)

A certain amount of degradation may be caused by different environmental factors and

meteorological conditions depending on the structure of the PV module. The module degradation factor (MDF) given in Eq. 1 was used to define the amount of degradation. This value can be used for

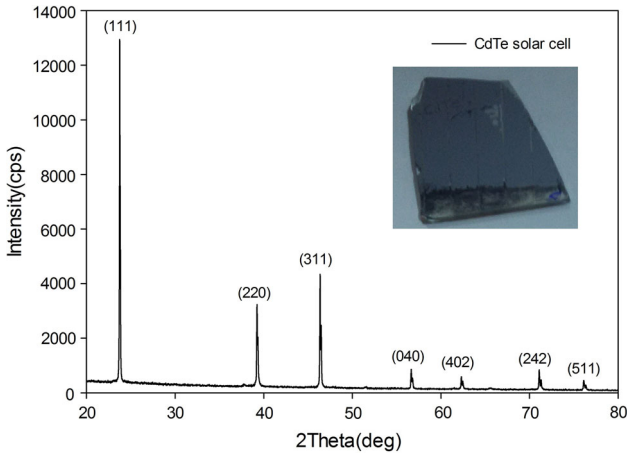

Fig. 9. XRD pattern of an undamaged part of CdTe thin-film PV module as shown in the inset.

different types of modules facing failures at different times and at different scales. When performing the MDF calculation, the short-circuit current of the ideal module, which is undamaged, and the short-circuit current of the degraded or damaged module are considered as the reference parameters. Depending on the amount of degradation, the series resistance effect within the terminals of the module starts prevailing, resulting in a reduction of the short-circuit current of the PV module.[5] Thus, knowing the MDF of a module provides an index about the specific module that can be used to easily classify the modules in a string or even in a large-scale installation.

$$\%\mathrm{MDF} = \left(1 - I_{\mathrm{SC}_{(\mathrm{Degraded})}} / I_{\mathrm{SC}_{(\mathrm{Ideal})}}\right) \times 100 \qquad (1)$$

Here, %MDF is the module degradation factor, $I_{\mathrm{SC(Degraded)}}$ is the short-circuit current of degraded module, and $I_{\mathrm{SC(Ideal)}}$ is the short-circuit current of an ideal (undamaged) module.

Table II presents the parameters for the determination of the MDF. All the values in Table II were

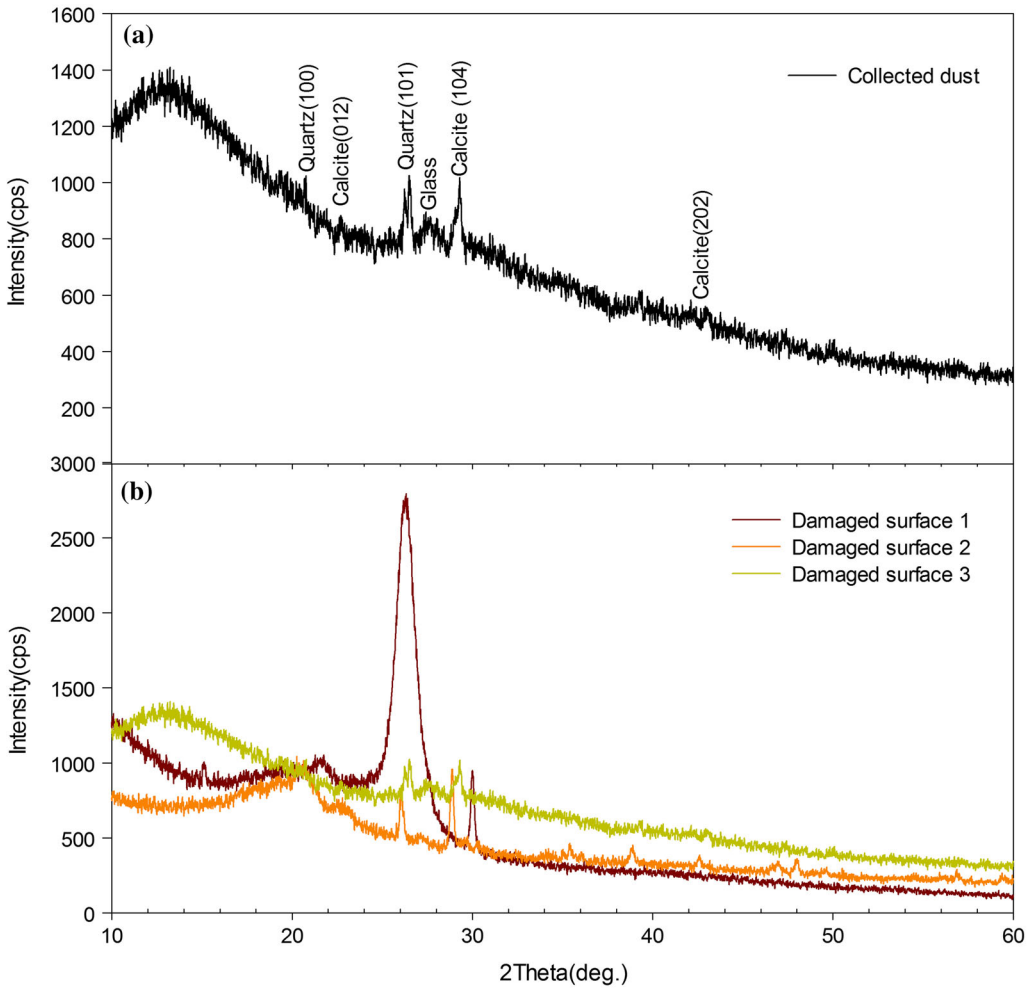

Fig. 10. XRD patterns of (a) dust collected on CdTe PV surface, and (b) damaged CdTe PV surfaces.

Table II. Catalogue, measured, and calculated parameters of thin-film PV modules under evaluation

PV module parameters		CdTe	CIS
Catalogue parameters at 800 W/m^2	Nominal power (W)	49.5	40.3
	Current at P_{MPP} (A)	1.63	2.16
	Short-circuit current (A)	1.98	1.93
Measured parameters	Ambient temperature (°C)	27	27
	Solar radiation (W/m^2)	800	800
	Degraded short-circuit current (A)	1.693	1.520
Calculated parameters	%MDF	14.49	21.24

obtained under normal operating cell temperature conditions at 800 W/m^2 using the catalogue values for the modules.[25,26] In our exploration, CdTe and CIS modules were used. During the measurements, the ambient temperature was measured to be 27°C and the solar radiation value was 800 W/m^2. Table II also tabulates the short-circuit currents of the ideal and degraded modules in the strings. A significant reduction in the currents was observed for both modules after the degradation caused by the module failures. The last row in Table II presents the %MDF values based on the measured short-circuit currents.

CONCLUSIONS

In this study, the types of failures occurring in CdTe and CIS thin-film PV modules were investigated, and the effects of these failures on performance, including the efficiency and power generation capability, were analyzed. Two comparable PV strings with identical power ratings and inclination angles were built using CdTe and CIS thin-film PV modules for a rooftop application at Gazi University Golbasi Campus, Ankara, Turkey. During the 3.5-year exploration, we observed that the effects of the climate and environmental conditions differed for the two types of module strings, with different types of failures detected depending on the material. An important difference in the degradation factors of the materials was also observed. The major failures that we were able to accurately detect were delamination, micro-cracks, corrosion, and hot-spot defects. Micro-cracks and delamination faults yielded a degradation factor of 21.24% for the CIS modules and a degradation factor of 14.49% for the CdTe modules. Therefore, the failed modules in the CIS string resulted in an average loss in the generated power reaching up to 31.5%; in contrast, this value was only 21.7% for the CdTe string. The structural defects in the modules were analyzed using XRD. The existence of a large amount of dust containing calcite and quartz on the damaged surfaces indicated the occurrence of structural damage. The delamination effects on the CIS modules were detected using IR analysis. It is important to note that a fault in a single module in a row not only causes a decrease in power in that module but also negatively affects the entire string. When the measured data for the PV modules of the CdTe structure were examined, it was observed that the micro-crack failures encountered in these modules caused less efficiency loss. However, in autumn and winter months (especially in foggy and rainy conditions), an earth-leakage fault of the entire system could occur because of moisture entering these micro-cracks in the damaged modules. This fault caused the inverters to completely cut off the power generation, and the module string did not reconnect to the grid until the moisture in the cracks was dried. In conclusion, the performance of CIS and CdTe modules is affected by meteorological conditions; these factors should thus be evaluated before implementing a module design to achieve the most efficient and cost-effective power generation.

ACKNOWLEDGMENTS

This work was conducted in Gazi University Campus and utilized the PV modules in the solar power plant installed within the scope of a Gazi Technopark SAN-TEZ project. The authors would like to thank the management of Gazi Technopark and the relevant staff in Gazi University. We thank Tiffany Jain, M.S., from Edanz Group (www.edanzediting.com/ac) for editing a draft of this manuscript.

REFERENCES

1. International Energy Agency, Monthly electricity statistics (2018), http://www.iea.org/media/statistics/surveys/electricity/mes.pdf. Accessed 20 May 2018.
2. İ. Çetinbaş, B. Tamyürek, and M. Demirtaş, *EMO Bilimsel Dergi* 8, 41 (2018).
3. Y. Min, J. RokLim, J.W. Ko, and H.K. Ahn, *J. Photovolt.* 7, 1488 (2017).
4. A. Bosio, G. Rosa, and N. Romeo, *Sol. Energy* 175, 31 (2018).
5. A. Dhoke, R. Sharma, and T.K. Saha, *Sol. Energy* 160, 360 (2018).
6. A. Ndiaye, A. Charki, A. Kobi, C.M.F. Kébé, P.A. Ndiaye, and V. Sambou, *Sol. Energy* 96, 140 (2013).
7. International Energy Agency, Review of failures of photovoltaic modules (2014), http://iea-pvps.org/fileadmin/dam/intranet/ExCo/IEA-PVPS_T13-01_2014_Review_of_Failures_of_Photovoltaic_Modules_Final.pdf. Accessed 20 May 2018.
8. D.C. Jordan, S.R. Kurtz, K. VanSant, and J. Newmiller, *Prog. Photovolt.: Res. Appl.* 24, 978 (2016).
9. W. Muehleisen, G.C. Eder, Y. Voronko, M. Spielberger, H. Sonnleitner, K. Knoebl, R. Ebner, G. Ujvari, and C. Hirschl, *Renew. Energy* 118, 138 (2018).

10. S.S. Chandel, M.N. Naik, V. Sharma, and R. Chandel, *Renew. Energy* 78, 193 (2015).
11. A. Bouraiou, M. Hamouda, A. Chaker, A. Neçaibia, M. Mostefaoui, N. Boutasseta, A. Ziane, R. Dabou, N. Sahouane, and S. Lachtar, *Sol. Energy* 159, 475 (2018).
12. F. Bandou, A.H. Arab, M.S. Belkaid, P.O. Logerais, O. Riou, and A. Charki, *Int. J. Hydrog. Energy* 40, 13839 (2015).
13. E. Andenæs, B.P. Jelle, K. Ramlo, T. Kolås, J. Selj, and S.E. Foss, *Sol. Energy* 159, 318 (2018).
14. S. Silvestre, S. Kichou, L. Guglielminotti, G. Nofuentes, and M. Alonso-Abella, *Sol. Energy* (2016). https://doi.org/10.1016/j.solener.2016.10.030.
15. A. Tahri, S. Silvestre, F. Tahri, S. Benlebna, and A. Chouder, *Sol. Energy* 157, 587 (2017).
16. M. Demirtaş, B. Tamyürek, E. Kurt, and İ. Çetinbaş, in *Proceedings of ECRES* (2018).
17. N. Kahoul, M. Houabes, and M. Sadok, *Energy Convers. Manag.* 82, 320 (2014).
18. D.A. Quansah and M.S. Adaramola, *Int. J. Hydrog. EnergY* 43, 3092 (2018).
19. NREL, Cadmium telluride solar cells, https://www.nrel.gov/pv/cadmium-telluride-solar-cells.html. Accessed 20 Sept 2018.
20. S.J. Ikhmayies, *J. Energy Syst.* (2017), https://doi.org/10.30521/jes.355507.
21. M.A. Green, Y. Hishikawa, W.D. Dunlop, D.H. Levi, J. Hohl-Ebinger, and A.W.Y. Ho-Baillie, *Prog. Photovolt. Res. Appl.* 26, 3 (2018).
22. V.K. Nagar and S.K. Srivastava, *IJIREEICE* 4, 235 (2016).
23. T. Pavlović, D. Milosavljević, I. Radonjić, L. Pantić, A. Radivojević, and M. Pavlović, *Renew. Sust. Energy Rev.* 20, 201 (2013).
24. Q. Li, K. Chi, Y. Mu, W. Zhang, H. Yang, W. Fu, and L. Zhou, *Mater. Lett.* 117, 225 (2014).
25. Bosch Obsidian solar module datasheet, http://www.bosch-solarenergy.com/media/sede/kundendienst_3/produkte/cis_solarmodule/eng/1-bosch_solar_modules_obsidian_2010-09-en_datasheet.pdf. Accessed 30 Jan 2019.
26. Abound AB1 series solar module datasheet, http://sunelec.com/Specs/Abound%20AB-1.pdf. Accessed 30 Jan 2019.

Publisher's Note Springer Nature remains neutral with regard to jurisdictional claims in published maps and institutional affiliations.